

Therapeutic effects of dipyridamole on COVID-19 patients with coagulation dysfunction

Xiaoyan Liu^{1#}, Zhe Li^{2#}, Shuai Liu^{1,3#}, Zhanghua Chen^{4,5#}, Jing Sun^{6#}, Zhiyao Zhao^{4#}, Yi-you Huang^{2#}, Qingling Zhang^{6#}, Jun Wang⁴, Yinyi Shi³, Yanhui Xu⁴, , Huifang Xian⁴, Rongli Fang⁴, Fan Bai⁵, Changxing Ou⁶, Bei Xiong¹, Andrew M Lew⁷, Jun Cui⁸, Hui Huang⁹, Jincun Zhao^{6*}, Xuechuan Hong^{10,11*}, Yuxia Zhang^{4*}, Fuling Zhou^{1*}, and Hai-Bin Luo^{2*}

¹Department of Hematology, Zhongnan Hospital of Wuhan University, Wuhan, 430071, China

²School of Pharmaceutical Sciences, Sun Yat-sen University, Guangzhou, 510006, P. R. China

³Dawu County People's Hospital, Xiaogan City, 432826, China

⁴Guangzhou Institute of Pediatrics, Guangzhou Women and Children's Medical Center, State Key Laboratory of Respiratory Diseases, Guangzhou Medical University, Guangzhou, 510623, China

⁵Biomedical Pioneering Innovation Center (BIOPIC), School of Life Sciences, Peking University, Beijing, 100871, China

⁶Department of Allergy and Clinical Immunology, State Key Laboratory of Respiratory Diseases, National Clinical Research Center for Respiratory Disease, Guangzhou Institute of Respiratory Health, The First Affiliated Hospital of Guangzhou Medical University. 151 Yanjiang Road, Guangzhou, 510120, China

⁷Walter and Eliza Hall Institute of Medical Research and Department of Microbiology & Immunology, University of Melbourne, Parkville, Vic, 3052, Australia

⁸School of Life Sciences, Sun Yat-sen University, Guangzhou, Guangdong, 510006, China

⁹ Cardiovascular Department, The Eighth Affiliated Hospital, Sun Yat-sen University, Shenzhen, 518000, China

NOTE: This preprint reports new research that has not been certified by peer review and should not be used to guide clinical practice.

¹⁰State Key Laboratory of Virology, College of Science, Innovation Center for Traditional Tibetan Medicine Modernization and Quality Control, Medical College, Tibet University, Lhasa, 850000, China

¹¹Key Laboratory of Combinatorial Biosynthesis and Drug Discovery (MOE), Hubei Province Engineering and Technology Research Center for Fluorinated Pharmaceuticals, Wuhan University School of Pharmaceutical Sciences, Wuhan, 430071, China

#Joint first authors.

***Corresponding authors**

1) Prof. Hai-Bin Luo: School of Pharmaceutical Sciences, Sun Yat-sen University, Guangzhou, 510006, China. E-mail: luohb77@mail.sysu.edu.cn

2) Prof. Fuling Zhou: Department of Hematology, Zhongnan Hospital of Wuhan University, Wuhan, 430071, China. E-mail: zhoufuling@whu.edu.cn

3) Prof. Yuxia Zhang: Guangzhou Institute of Pediatrics, Guangzhou Women and Children's Medical Center, State Key Laboratory of Respiratory Diseases, Guangzhou Medical University, Guangzhou, 510623, China. E-mail: yuxia.zhang@gwcmc.org

4) Prof. Jincun Zhao: State Key Laboratory of Respiratory Diseases, Guangzhou Institute of Respiratory Health, The First Affiliated Hospital of Guangzhou Medical University, Guangzhou, 510120, China. E-mail: zhaojincun@gird.cn

5) Prof. Xuechuan Hong: State Key Laboratory of Virology, College of Science, Innovation Center for Traditional Tibetan Medicine Modernization and Quality Control, Medical College, Tibet University, Lhasa, 850000, China. E-mail: xhy78@whu.edu.cn

Abstract: The human coronavirus HCoV-19 infection can cause acute respiratory distress syndrome (ARDS), hypercoagulability, hypertension, extrapulmonary multiorgan dysfunction. Effective antiviral and anti-coagulation agents with safe clinical profiles are urgently needed to improve the overall prognosis. We screened an FDA approved drug library and found that an anticoagulant agent dipyridamole (DIP) suppressed HCoV-19 replication at an EC50 of 100 nM *in vitro*. It also elicited potent type I interferon responses and ameliorated lung pathology in a viral pneumonia model. In analysis of twelve HCoV-19 infected patients with prophylactic anti-coagulation therapy, we found that DIP supplementation was associated with significantly increased platelet and lymphocyte counts and decreased D-dimer levels in comparison to control patients. Two weeks after initiation of DIP treatment, 3 of the 6 severe cases (60%) and all 4 of the mild cases (100%) were discharged from the hospital. One critically ill patient with extremely high levels of D-dimer and lymphopenia at the time of receiving DIP passed away. All other patients were in clinical remission. In summary, HCoV-19 infected patients could potentially benefit from DIP adjunctive therapy by reducing viral replication, suppressing hypercoagulability and enhancing immune recovery. Larger scale clinical trials of DIP are needed to validate these therapeutic effects.

Keyword: Dipyridamole, HCoV-19, Pneumonia, Treatment, D-dimer

Introduction

The novel coronavirus HCoV-19 (also known as SARS-CoV-2) outbreak had emerged from Wuhan, Hubei Province, China in December 2019.^{1,2} As of February 24, there had been 77,787 confirmed COVID-19 cases including 2,666 deaths in China. Over 2,500 infections have also been reported in

28 other countries, such as Japan, South Korea, Italy, Singapore, Iran, Thailand, and U.S.A; this rapid spread threatens to become a pandemic. To date, no agents have been reported to be effective against this infection. Identification of readily available drugs for repurpose in COVID-19 therapy avail a relatively rapid way to clinical treatment.³

HCoV-19, together with SARS-CoV and MERS-CoV, belong to the *Beta-coronavirus* genus, which are enveloped, positive-stranded RNA viruses with approximately 30,000 nucleotides.^{4,5} Angiotensin I converting enzyme 2 (ACE2) is the receptor that engages the Spike surface glycoprotein of SARS-CoV and HCoV-19.^{6,7} ACE2 is expressed in many organs, including the lung, heart, kidney, and intestine. Notably, in experimental models of SARS-CoV infection, Spike protein engagement decreases ACE2 expression and activates the renin-angiotensin system (RAS).⁶ RAS activation promotes platelet adhesion and aggregation and increases the risk for pulmonary embolism, hypertension and fibrosis.⁸⁻¹¹ It also accelerates cardiac and kidney injury by increasing local angiotensin II concentrations.¹²⁻¹⁴ Apart from affecting the classic RAS pathway, ACE2 deficiency in the intestine is associated with malnutrition and colonic inflammation.¹⁵

Infection from SARS-CoV can result in severe lymphopenia, prolonged coagulation profiles, lethal acute respiratory distress syndrome (ARDS), watery diarrhea, cardiac disease and sudden death.^{9,16-18} Many of these features have also been reported for COVID-19: prolonged coagulation profiles, elevated D-dimer levels, severe lymphopenia, ARDS, hypertension, and acute heart injury in ICU-admitted patients.^{2,19} Given that angiotensin II levels were highly elevated in the HCoV-19 infected patients,²⁰ RAS was likely activated in HCoV-19 infected patients. Thus, prophylactic anti-coagulation therapy should be considered for mollifying the multi-organ damage during severe COVID-19.

After viral entry to the host cells, the coronavirus messenger RNA is first translated to yield the polyproteins, which are subsequently cleaved by two viral proteinases, 3C-like protease (3CLP, aka nsp5 or Mpro) and papain-like protease (PLP, or nsp3), to yield non-structural proteins essential for viral replication.²¹ Inhibitors that suppress the activity of these proteases may inhibit viral replication and offer a revenue for the HCoV-19 therapy.

Dipyridamole (DIP) is an antiplatelet agent and acts as a phosphodiesterase (PDE) inhibitor that increases intracellular cAMP/cGMP.²² Apart from the well-known antiplatelet function, DIP may provide additional therapeutic benefits to COVID-19 patients. First, published studies,²³⁻²⁸ including clinical trials conducted in China,²⁹⁻³¹ have demonstrated that DIP has a broad spectrum antiviral activity, particularly efficacious against the positive-stranded RNA viruses.²⁴ Second, it suppresses inflammation and promotes mucosal healing.³² Third, as a pan-PDE inhibitor, DIP may prevent acute injury and progressive fibrosis of the lung, heart, liver, and kidney.³³ Here we provide three levels of evidence advocating DIP as a therapy. *In silico and in vitro*, we demonstrated that DIP possessed anti- HCoV-19 effects. In a VSV-induced pneumonia model, we also confirmed that DIP elicited potent antiviral immunity and significantly improved the survival rate. In a small clinical cohort, we found that DIP adjunctive therapy led to increased circulating lymphocyte and platelet counts and lowered D-dimer levels, and markedly improved clinical outcomes.

Methods

Free energy perturbation and surface plasmon resonance (SPR) assay

We virtually screened an FDA-approved drug database using the HCoV-19 protease Mpro as a target and validated the binding affinity by the SPR assay. DIP (PubChem CID: 3108, Figure S1) was identified as a lead drug. In order to obtain the binding pattern and calculate the binding free energy

between DIP and Mpro, DIP was firstly docked onto Mpro by using Glide, and the optimal binding pose was further assessed by absolute binding free energy calculation with free energy perturbation.³⁴ The calculations were carried out in Gromacs 2019, and the thermodynamic cycle and procedure was similar to that used by Matteo et al.³⁵ In the calculation, the ligand electrostatic and van der Waals interactions were decoupled using a linear alchemical pathway with $\Delta\lambda = 0.10$ for the van der Waals and $\Delta\lambda = 0.20$ for electrostatic interactions. To add the restraints, 12 λ values were used. Therefore, a total of 28 windows for complex and 16 windows for ligand systems were employed, and 4 ns simulations were performed for each window. The relative position restraints consist of one distance, two angles, and three dihedrals harmonic potentials with a force constant of 10 kcal/mol/Å² [rad²]. The distance and angles for the restraints were determined by the values of the last 2 ns of the 4 ns preliminary MD simulations. The sampled ΔU in the simulations were fitted by Gaussian algorithms and the free energy estimates were obtained by using the Bennet acceptance ratio (BAR) method.³⁶

The pGEX4T1-Mpro plasmid was constructed (Atagenix, Wuhan) and transfected the E. coli strain BL21 (Codonplus, Stratagene). GST-tagged protein was purified by GST-glutathione affinity chromatography and cleaved with FXa. The purity of recombinant protein was greater than 95% as judged by SDS-PAGE. The binding of DIP to Mpro was measured by the Biacore 8K system (GE healthcare) at 25 °C. Mpro was immobilized on a CM5 chip surface via covalent linkage to Mpro N-terminus. First, the CM5 chip was activated using 1:4 *N*-hydroxysuccinimide (NHS)/1-ethyl-3-(3-dimethylaminopropyl) carbodiimide (EDC) at the flow rate of 10 μL/min for 7 min. Then, Mpro (90 μg/mL) in 10 mM acetate buffer (pH 4.5) was passed over separate flow cells

at 10 μ L/min for 3 min (1800 response units), which followed by a blocking step using ethanolamine (1 M, pH 8.5) at 10 μ L/min for 7 min. Binding studies were performed by passing 5-80 μ M of DIP over the immobilized Mpro at the flow rate of 30 μ L/min and the contact time was set to be 200 s. A sample volume of 120 μ L DIP in running buffer was injected into the flow cell and the bound ligand was washed by running buffer which contained 10 mM phosphate, 137 mM NaCl, 2.7 mM KCl, pH 7.4, and 0.5% DMSO.

Fluorescent focus assay

Vero E6 cells were seeded in 96-well plates and treated with different dosages of dipyridamole or chloroquine for an hour before infected with HCoV-19. After 24 hours of incubation, cells were fixed and permeabilized with Cytofix/Cytoperm (BD), incubated with a rabbit anti-HCoV-19 nucleocapsid protein polyclonal antibody (Sino Biological), followed by a HRP-labelled goat anti-rabbit secondary antibody (Jackson). The foci were visualized by TRUEBlue reagent. Foci in infected cells were counted with a ELISPOT reader. Viral titers were calculated as foci forming units (FFU) per ml.

RNA extraction and quantitative real-time PCR

Total cellular RNA was isolated by TRIzol reagent (Invitrogen) and reverse transcription was performed using a reverse transcription kit (Vazyme). We performed real-time PCR with SYBR Green qPCR Mix (GenStar). Data were normalized to the *RPL13A* gene and relative abundance of transcripts was calculated by the *Ct* models. Following primers were used for real-time PCR:

IFN- β forward primer: 5'CAGCAATTTTCAGTGTGTCAGAAGC3';

162 *IFN-β* reverse primer: 5'TCATCCTGTCCTTGAGGCAGT3';
 163 *ISG15* forward primer: 5' TCCTGGTGAGGAATAACAAGGG3';
 164 *ISG15* reverse primer: 5' GTCAGCCAGAACAGGTCGTC3';
 165 *IFIT1* forward primer: 5' TCAGGTCAAGGATAGTCTGGAG3';
 166 *IFIT1* reverse primer: 5' AGGTTGTGTATTCCCACACTGTA3'.
 167 *RPL13A* forward primer: 5'GCCATCGTGGCTAAACAGGTA3'
 168 *RPL13A* reverse primer: 5'GTTGGTGTTCATCCGCTTGC3'

169

170 Immunoblotting

171 Whole-cell extracts were eluted with 5×SDS Loading Buffer and then resolved by SDS-PAGE. The
 172 resolved protein bands were electro-transferred to polyvinylidene fluoride membranes for further
 173 antibody incubation and detection. The antibodies against TBK1 [TBK1/NAK (D1B4) Rabbit mAb
 174 #3504, Phospho-TBK1/NAK (Ser172) (D52C2) XP® Rabbit mAb #5483] and IRF3 [IRF-3 (D83B9)
 175 Rabbit mAb #4302, Phospho-IRF-3 (Ser386) (E7J8G) XP® Rabbit mAb #37829] were purchased
 176 from Cell Signaling Technology and anti-β-actin (A1978) were purchased from Sigma.

177

178 VSV-induced viral pneumonia model

179 C57/BL-6J mice were obtained from the Guangdong Medical Laboratory Animal Center. Six-week
 180 old female mice were intravenous injected with VSV (10⁸ PFU/g) and followed with DIP (35 mg/kg;
 181 intraperitoneal injection, i.p; twice/day) treatment for 5 days. Survival curve was measured. Mice
 182 were sacrificed at Day 4 for histology examination by hematoxylin-eosin (H&E) staining. The study
 183 procedure was approved by Animal Ethics Committee of Guangzhou Medical University.

184

185 **Patients and study variables**

186 As of February 8, 2020, 124 confirmed COVID-19 cases had been identified from Zhongnan
 187 Hospital of Wuhan University (**Table S1**). All patients met the diagnostic criteria of "Diagnosis and
 188 Treatment Scheme of Novel Coronavirus–Infected Pneumonia (trial 6th)" formulated by the General
 189 Office of National Health Committee.³⁷ A retrospective review of the medical records of these
 190 patients was conducted to retrieve coagulation indexes and platelet parameters, including
 191 prothrombin time (PT), activated partial thromboplastin time (APTT), plasma fibrinogen (FIB),
 192 D-dimer, platelet (PLT) count, and mean platelet volume (MPV). Systemic inflammation was
 193 assessed according to the C-reactive protein (CRP), procalcitonin (PCT), and interleukin 6 (IL-6)
 194 levels.¹²

195

196 **Study design**

197 Patients were enrolled from the isolation ward in Dawu County People's Hospital, a medical
 198 treatment alliance of Zhongnan Hospital, Hubei province in China, from Jan 23, 2020 to Feb 22,
 199 2020 to determine the effect of DIP to improve the coagulation profile. The condition of the patients
 200 was monitored daily by attending physicians. Routine laboratory test of the coagulation variables,
 201 blood indexes, liver and kidney function indices, and chest CT were carried out before, during, and
 202 after the treatment. Clinical symptoms and laboratory data were independently validated by two
 203 independent investigators for assurance of data accuracy. The diagnosis of severe case was made if
 204 patients met any of the following criteria: (1) respiratory rate ≥ 30 breaths/min; (2) SpO₂ $\leq 93\%$
 205 while breathing room air; (3) PaO₂/FiO₂ ≤ 300 mmHg. A critically ill case was diagnosed if any of

the following criteria was met: (1) respiratory failure which requiring mechanical ventilation; (2) shock; (3) combined with other organ failure, need to be admitted to ICU. The Ethics Committee from Dawu County People's Hospital approved the study. All patients signed informed consents.

Treatment procedures

Anticoagulant therapy was provided via oral DIP tablets. The daily treatment protocol comprised of 150 mg in three separate doses for seven consecutive days. All patients were monitored daily for possible adverse events. All patients received antiviral (ribavirin, 0.5g, Q12h), corticoid (methylprednisolone sodium succinate, 40 mg, qd), oxygen therapy, and nutritional support as necessary.

Statistical analysis

Statistical analyses and graphics production were performed using R v3.5.3 (Foundation for Statistical Computing) and GraphPad Prism 8. Categorical variables were described as frequencies or percentages, and continuous variables were shown as mean with standard deviation/error or median with interquartile range. Comparison for two independent groups was conducted using Student's *t* test (for normally distributed data) or Mann-Whitney test (for non-normally distributed data). *P* < 0.05 was considered statistically significant. Detailed descriptions of data comparison and statistical tests were specified in the figure legends.

Results

DIP suppresses HCoV-19 replication in Vero E6 cells

We virtually screened an FDA approved drug library and found that DIP bound to the HCoV-19 protease Mpro (**Figure S1**). Hydrophobic and hydrogen bond (H-bond) interactions are the main driving forces for the binding between DIP and Mpro. According to the free energy perturbation calculation, the binding free energy of ΔG_{pred} was -6.34 kcal/mol. An SPR assay was carried out to validate the *in silico* result. This has revealed that DIP bound to Mpro with an experimentally confirmed affinity of 34 μM ($K_{D,eq}$) (**Figure 1A-B**).

To demonstrate directly that DIP suppresses HCoV-19 replication, we measured the viral titers using a susceptible cell line, the Vero E6 cells. Chloroquine was used as a positive control.^{38,39} Remarkably, at 0.1 μM DIP suppressed more than 50% of HCoV-19 replication (**Figure 1C**). Human DIP administration can achieve a 3 μM serum concentration.⁴⁰ Thus, therapeutic dosages of DIP may effectively suppress HCoV-19 replication in the infected patients. Notably, however, the dose-dependent suppressive effect of dipyrindamole was less apparent in comparison to Chloroquine, which suggested that DIP may employ a different mode of suppression.

DIP promotes type I interferon (IFN) responses and protect mice from viral pneumonia

Published studies have shown that DIP possessed broad spectrum activity to a wide range of viruses, indicating that it may elicit antiviral immunity from the host cells. We examined these using two single-stranded RNA viruses (Sendai virus, SeV and Vesicular stomatitis virus, VSV), as well as intracellular poly (I:C) that stimulates the RIG-I and MDA5 mediated IFN immunity, in the human

lung epithelial cell line A549 cells.^{41,42} Our results demonstrated that DIP (5 μ M) treatment significantly increased *IFNB*, *IFIT1*, and *ISG15* messenger RNA expression and promoted IFN- β secretion (**Figure 2A**) by increasing TBK1 and IRF3 phosphorylation (**Figure 2B**).

To validate the antiviral effects of DIP *in vivo*, we established a VSV-induced pneumonia model. DIP administration significantly prolonged the survival rate of VSV-infected mice (**Figure 2C**), and substantially alleviated pulmonary pathology (**Figure 2D**). Thus, therapeutic doses of DIP can elicit potent and broad-spectrum antiviral immunity to single-stranded RNA viruses.

A remarkable improvement of coagulation profile in COVID-19 patients receiving DIP adjunctive therapy

To assess the coagulation profile, we first retrospectively analyzed a randomly collected cohort of 124 COVID-19 patients (**Table S1**). Decreased platelet counts were observed in 25 (20.2%) patients, prolonged prothrombin time (PT) was observed in 77 (62.1%) patients, fibrinogen (FIB) levels were increased in 27 (21.8%) patients, and D-dimer levels were increased in 26 (21.0%) patients. This suggest that hypercoagulability is common in COVID-19 patients.

To evaluate DIP as a therapy to reduce the risk of hypercoagulability, 22 additional patients including 10 control patients and 12 patients who received DIP were recruited. Baseline characteristics of the two groups were similar (**Table 1**). The average ages of the patients were 53 and 58 years in the DIP group and the control group, respectively. All patients manifested cough and most of them felt shortness of breath, and 60.0% patients had nausea and vomiting. Chest CT scan revealed bilateral

pneumonia in all patients. Comorbidities, including diabetes mellitus, cardiovascular and cerebrovascular diseases, were found in 4 and 5 of the patients from the DIP and control group, respectively. All patients received ribavirin, glucocorticoids, and oxygen therapy, but none received antifungal treatment. Other treatment included mechanical ventilation (16.7% vs 10.0%), antibiotics (33.3% vs 30.0%), and intravenous immunoglobulin (16.7% vs 20.0%) in the DIP group and the control group, respectively.

Two weeks after initiation of DIP treatment, 3 of the 6 severe cases (50%) and all 4 of the mild cases (100%) were discharged from the hospital. One of the critically ill patient with extremely high levels of D-dimer and lymphopenia at the time of receiving DIP passed away. All other patients were in clinical remission. In comparison, the discharge and remission rates of the mild and severe cases were inferior in the control patients (**Table 2**).

The baseline temperature was higher and the oxygenation status was worse in the DIP-treated group than those in the control group, however, temperature and oxygenation were stabilized in the mild and severe patients from both groups after one day of treatment (**Figure S2**). Furthermore, we observed a continuously increased trend in lymphocyte counts and significantly increased platelet numbers in patients receiving DIP treatment in comparison to the control group (**Figure 3A**). Given that lymphocytopenia and thrombocytopenia are common in the severe and critically ill patients, immune recovery may contribute to infection resolution in DIP-treated patients. It should be noted that 4 patients from the DIP-treatment group and 2 patients from the control group had increased baseline levels of D-dimer when they were admitted to the hospital (**Table 1**). We measured dynamic

changes in reference to the respective baseline levels for all patients, and found that the levels of D-dimer continuously rose in the control group, whereas they were decreased and stabilized in the DIP-treated group (**Figure 3A, Figure S2**).

We then examined the two critically ill patients who received DIP adjunctive therapy. A 70-year-old man with very low oxygen saturation and has suffered from hypoxia and multiorgan dysfunction at hospital administration has passed away. He had extremely high levels of D-dimer (16.2 mg/L) and very low lymphocyte count ($0.37 \times 10^9/L$) at the time of receiving DIP adjunctive therapy. His oxygen saturation remained low and has unfortunately passed away 5 days since initiation of DIP treatment. In contrast, the other severely ill patient also had very low oxygen saturation and high D-dimer level (8.83 mg/L) at administration. His D-dimer level had gone up to as high as 15.72 mg/L, but gradually declined to 3.69 mg/L following DIP adjunctive therapy. The patient has since been in clinical remission. This reinforces that high levels of D-dimer and low lymphocyte counts are associated with poor prognosis and suggest that that DIP treatment should be initiated before the progression to critical illness (**Figure 3B**).

All patients had chest CT scans and showed typical multiple patchy ground-glass shadows in the lungs before the treatment. In the DIP treated patients, the lesions had varied degree of absorption. Typical findings following DIP treatment was illustrated in one of the severe COVID-19 patient who had taken sequential CT scans (**Figure 4**).

Discussion

Despite the enormous threat of HCoV-19, no drugs have been claimed to be effective including the existing drugs used to treat other viruses. In reference to SARS-CoV- infection, we hypothesized that the HCoV-19 Spike protein engagement may activate RAS in the lung.^{6,43} This hypothesis was supported by published clinical characteristics and biochemical indices of the severe and critically ill COVID-19 patients, who showed ARDS, hypertension, acute heart, kidney injury, and positive D-dimer results.^{2,19,20} In searching for available anticoagulants, we focused on DIP because of its broad-spectrum antiviral, anti-inflammatory, and anti-fibrotic effects. We confirmed that DIP possessed potent antiviral immunity to single-stranded RNA viruses *in vitro*, and in a VSV-induced viral pneumonia model *in vivo*. Most importantly, a laboratory confirmed EC₅₀ of 0.1 μ M to suppress HCoV-19 replication highly suggested that the therapeutic dosage of DIP may potentiate effective antiviral responses in infected patients . These findings are in concordance with the overall remarkable outcomes in patients receiving one week of DIP adjunctive therapy, seven of the twelve patients were discharged from the hospital and four achieved clinical remission.

We found that DIP adjunctive treatment was effective in preventing hypercoagulability if applied early in the severe COVID-19 patients. DIP treatment blunted the increase in D-dimer levels and increased circulating platelet and leucocytes counts, and thus was associated with overall remarkable clinical cure and remission rates. High levels of D-dimer closely correlated with pulmonary embolism,⁴⁴ vascular thrombosis, and renal dysfunction.⁴⁵ It is an important prognostic factor of whether ICU-patients may recover from severe infections.^{46,47} As such, the antiviral, anti-inflammatory, and anti-hypercoagulability effects of DIP could reduce the risk of micro-vascular

thrombosis in HCoV-19 infected patients. This could in turn improve vascular circulation and restore vital functions of important organs such as heart and kidney.

In summary, we suggest anti-coagulant therapy for COVID-19 patients with early signs of elevated D-dimer levels. DIP is an attractive anti-coagulant adjunctive therapy due to its safe clinical profile as an anti-platelet agent. It also holds additional benefits as a pan-PDE inhibitor in eliciting broad-spectrum antiviral immunity, as well as anti-inflammatory and anti-fibrotic effects. Moreover, the wide availability, safety and affordability of DIP argue for further investigation into its therapeutic use in COVID-19, particularly in the event of its rapid spread into the developing countries.

Contributors

JZ, XH, YZ, FZ, and HBL co-designed the study and co-led overall data interpretation. ZL led the virtual screening, YH led the SPR analysis, ZC, ZZ, JW, YX, JL, HX, RF, FB, CJ, HH, and CO also participated in study design and performed *in vivo* and *in vitro* studies. XL, SL, YS, BX, XH, and FZ led the clinical analysis. XL, SL, YS, BX, XH, and FZ participated in data collection. ZC participated in data analysis. XL, SL, and ZC produced the tables and figures. AML reviewed the manuscript. YZ and HBL drafted the manuscript with significant input from JZ, XH, and FZ. All authors interpreted the results and critically revised the manuscript for scientific content. All authors approved the final version of the Article.

Declaration of interests

HL, ZL, and YYH report grants from National Key R&D Program of China (2017YFB0202600), National Natural Science Foundation of China (8152204 and 21877134), and philanthropy donation from individuals. XL, SL, YS, BX, XH, and FZ report grants from Taikang Insurance Group Co., Ltd and Beijing Taikang Yicai Foundation, and philanthropy donation from individuals. YZ and XX report grants from National Natural Science Foundation of China (91742109, 31770978, and 81773674) and philanthropy donation from individuals during the conduct of the study. Other authors declare no competing interests.

Funding National Key R&D Program of China (2017YFB0202600), National Natural Science Foundation of China (91742109, 8152204, 31770978, 81773674, and 21877134), Taikang Insurance Group Co., Ltd and Beijing Taikang Yicai Foundation, and philanthropy donation from individuals. The funders had no roles in the design and execution of the study.

Acknowledgments

We cordially acknowledge Tencent Cloud, National Supercomputing centers in Guangzhou and Shenzhen, and SenseTime for providing HPC resources for virtual screening and free energy perturbation calculations. We cordially thank Prof. H. Ke at the University of North Carolina, Chapel Hill, for his help to improve our writing of this work.

Reference:

- Chen N, Zhou M, Dong X, et al. Epidemiological and clinical characteristics of 99 cases of 2019 novel coronavirus pneumonia in Wuhan, China: a descriptive study. *Lancet* 2020.
- Huang C, Wang Y, Li X, et al. Clinical features of patients infected with 2019 novel coronavirus in Wuhan, China. *Lancet* 2020.
- Holshue ML, DeBolt C, Lindquist S, et al. First Case of 2019 Novel Coronavirus in the United States. *N Engl J*

Med 2020.

4. Chan JF, Kok KH, Zhu Z, et al. Genomic characterization of the 2019 novel human-pathogenic coronavirus isolated from a patient with atypical pneumonia after visiting Wuhan. *Emerg Microbes Infect* 2020; **9**(1): 221-36.
5. Wu A, Peng Y, Huang B, et al. Genome Composition and Divergence of the Novel Coronavirus (2019-nCoV) Originating in China. *Cell Host Microbe* 2020.
6. Kuba K, Imai Y, Rao S, et al. A crucial role of angiotensin converting enzyme 2 (ACE2) in SARS coronavirus-induced lung injury. *Nat Med* 2005; **11**(8): 875-9.
7. Lu R, Zhao X, Li J, et al. Genomic characterisation and epidemiology of 2019 novel coronavirus: implications for virus origins and receptor binding. *Lancet* 2020.
8. Marshall RP. The pulmonary renin-angiotensin system. *Curr Pharm Des* 2003; **9**(9): 715-22.
9. Imai Y, Kuba K, Rao S, et al. Angiotensin-converting enzyme 2 protects from severe acute lung failure. *Nature* 2005; **436**(7047): 112-6.
10. Kalinowski L, Matys T, Chabielska E, Buczek W, Malinski T. Angiotensin II AT1 receptor antagonists inhibit platelet adhesion and aggregation by nitric oxide release. *Hypertension* 2002; **40**(4): 521-7.
11. Chung T, Connor D, Joseph J, et al. Platelet activation in acute pulmonary embolism. *J Thromb Haemost* 2007; **5**(5): 918-24.
12. Yamamoto K, Ohishi M, Katsuya T, et al. Deletion of angiotensin-converting enzyme 2 accelerates pressure overload-induced cardiac dysfunction by increasing local angiotensin II. *Hypertension* 2006; **47**(4): 718-26.
13. Oudit GY, Herzenberg AM, Kassiri Z, et al. Loss of angiotensin-converting enzyme-2 leads to the late development of angiotensin II-dependent glomerulosclerosis. *Am J Pathol* 2006; **168**(6): 1808-20.
14. Crackower MA, Sarao R, Oudit GY, et al. Angiotensin-converting enzyme 2 is an essential regulator of heart function. *Nature* 2002; **417**(6891): 822-8.
15. Hashimoto T, Perlot T, Rehman A, et al. ACE2 links amino acid malnutrition to microbial ecology and intestinal inflammation. *Nature* 2012; **487**(7408): 477-81.
16. Oudit GY, Kassiri Z, Jiang C, et al. SARS-coronavirus modulation of myocardial ACE2 expression and inflammation in patients with SARS. *Eur J Clin Invest* 2009; **39**(7): 618-25.
17. Peiris JS, Guan Y, Yuen KY. Severe acute respiratory syndrome. *Nat Med* 2004; **10**(12 Suppl): S88-97.
18. Peiris JS, Yuen KY, Osterhaus AD, Stohr K. The severe acute respiratory syndrome. *N Engl J Med* 2003; **349**(25): 2431-41.
19. Wang D, Hu B, Hu C, et al. Clinical Characteristics of 138 Hospitalized Patients With 2019 Novel Coronavirus-Infected Pneumonia in Wuhan, China. *JAMA* 2020.
20. Liu Y, Yang Y, Zhang C, et al. Clinical and biochemical indexes from 2019-nCoV infected patients linked to viral loads and lung injury. *Sci China Life Sci* 2020.
21. Adedeji AO, Sarafianos SG. Antiviral drugs specific for coronaviruses in preclinical development. *Curr Opin Virol* 2014; **8**: 45-53.
22. Gresele P, Momi S, Falcinelli E. Anti-platelet therapy: phosphodiesterase inhibitors. *Br J Clin Pharmacol* 2011; **72**(4): 634-46.
23. Tonew E, Indulen MK, Dzeguze DR. Antiviral action of dipyridamole and its derivatives against influenza virus A. *Acta Virol* 1982; **26**(3): 125-9.
24. Fata-Hartley CL, Palmenberg AC. Dipyridamole reversibly inhibits mengovirus RNA replication. *J Virol* 2005; **79**(17): 11062-70.
25. Tenser RB, Gaydos A, Hay KA. Inhibition of herpes simplex virus reactivation by dipyridamole. *Antimicrob Agents Chemother* 2001; **45**(12): 3657-9.
26. Szebeni J, Wahl SM, Popovic M, et al. Dipyridamole potentiates the inhibition by 3'-azido-3'-deoxythymidine and other dideoxynucleosides of human immunodeficiency virus replication in monocyte-macrophages. *Proc Natl*

Acad Sci U S A 1989; **86**(10): 3842-6.

27. Kozhukharova MS, Slepishkin AN, Radeva Kh T, Lavrukhina LA, Demidova SA. [Evaluation of dipyridamole efficacy as an agent for preventing acute respiratory viral diseases]. *Vopr Virusol* 1987; **32**(3): 294-7.

28. Kuzmov K, Galabov AS, Radeva K, Kozhukharova M, Milanov K. [Epidemiological trial of the prophylactic effectiveness of the interferon inducer dipyridamole with respect to influenza and acute respiratory diseases]. *Zh Mikrobiol Epidemiol Immunobiol* 1985; (6): 26-30.

29. Xie H. Efficacy of dipyridamole in the treatment of 116 children with acute upper respiratory tract infections. *Chinese Journal of School Doctor* 2010; **24**(12): 921-.

30. Hu X, Wang X. Treatment of viral upper respiratory tract infection in children with dipyridamole. *Chinese Journal of Hospital Pharmacy* 1995; (9).

31. Sui Y. Clinical observation of 45 cases of upper respiratory tract infection treated with dipyridamole. *The Medical Forum* 2014; **000**(032): 4360-1.

32. Huang B, Chen Z, Geng L, et al. Mucosal Profiling of Pediatric-Onset Colitis and IBD Reveals Common Pathogenics and Therapeutic Pathways. *Cell* 2019; **179**(5): 1160-76 e24.

33. Insel PA, Murray F, Yokoyama U, et al. cAMP and Epac in the regulation of tissue fibrosis. *Br J Pharmacol* 2012; **166**(2): 447-56.

34. Li Z, Huang Y, Wu Y, et al. Absolute Binding Free Energy Calculation and Design of a Subnanomolar Inhibitor of Phosphodiesterase-10. *J Med Chem* 2019; **62**(4): 2099-111.

35. Aldeghi M, Heifetz A, Bodkin MJ, Knapp S, Biggin PC. Accurate calculation of the absolute free energy of binding for drug molecules. *Chem Sci* 2016; **7**(1): 207-18.

36. HBennett C. Efficient estimation of free energy differences from Monte Carlo data. *Journal of Computational Physics* 1976; **22**(2): 245-68.

37. Committee GOoNH. Diagnosis and treatment scheme of novel coronavirus-infected pneumonia (trial version 6). <http://www.nhcgov.cn> 2020.

38. Vincent MJ, Bergeron E, Benjannet S, et al. Chloroquine is a potent inhibitor of SARS coronavirus infection and spread. *Viral J* 2005; **2**: 69.

39. Wang M, Cao R, Zhang L, et al. Remdesivir and chloroquine effectively inhibit the recently emerged novel coronavirus (2019-nCoV) in vitro. *Cell Res* 2020.

40. Serebruany V, Sabaeva E, Booze C, et al. Distribution of dipyridamole in blood components among post-stroke patients treated with extended release formulation. *Thromb Haemost* 2009; **102**(3): 538-43.

41. Sumpter R, Jr., Loo YM, Foy E, et al. Regulating intracellular antiviral defense and permissiveness to hepatitis C virus RNA replication through a cellular RNA helicase, RIG-I. *J Virol* 2005; **79**(5): 2689-99.

42. Loo YM, Gale M, Jr. Immune signaling by RIG-I-like receptors. *Immunity* 2011; **34**(5): 680-92.

43. Imai Y, Kuba K, Penninger JM. The discovery of angiotensin-converting enzyme 2 and its role in acute lung injury in mice. *Exp Physiol* 2008; **93**(5): 543-8.

44. Kline JA, Garrett JS, Sarmiento EJ, Strachan CC, Courtney DM. Over-Testing for Suspected Pulmonary Embolism in American Emergency Departments: The Continuing Epidemic. *Circ Cardiovasc Qual Outcomes* 2020; **13**(1): e005753.

45. Schefold JC, Gerber JL, Angehrn MC, et al. Renal Function-Adjusted D-Dimer Levels in Critically Ill Patients With Suspected Thromboembolism. *Crit Care Med* 2020.

46. Zhou J, Mao W, Shen L, Huang H. Plasma D-dimer as a novel biomarker for predicting poor outcomes in HBV-related decompensated cirrhosis. *Medicine (Baltimore)* 2019; **98**(52): e18527.

47. Adekanmbi O, Lakoh S. A favorable outcome of dengue hemorrhagic fever despite poor prognostic indices: a case report with a mix of classic and unusual clinical and laboratory features. *Pan Afr Med J* 2019; **34**: 74.

| Table 1. Baseline characteristics of enrolled patients | | |
|---|--------------------------------------|---------------------------------|
| Variable | Dipyridamole group (n=12) | Control group (n=10) |
| General Characteristic | | |
| Age (yr) — mean±sd (range) | 53±10 (32-69) | 58±15 (23-74) |
| Gender— male no. / female no. | 8 / 4 | 7 / 3 |
| Clinical variables | | |
| Cough— no. (%) | 12 (100.0%) | 10(100.0%) |
| Shortness of breath — no. (%) | 9 (75.0%) | 7(70.0%) |
| Nausea and vomiting— no. (%) | 7 (58.0%) | 6(60.0%) |
| Systolic blood pressure (mmHg) | 125±13(120-155) | 128±11(110-150) |
| — mean±sd (range) | /77±11(57-98) | /79±5(70-90) |
| Heart rate (beats/min) — mean±sd (range) | 87±7(75-100) | 83±12(59-101) |
| Partial pressure of oxygen (mmHg) | 86±12 (58-93) | 92±9 (76-96) |
| — mean±sd (range) | | |
| Laboratory values | | |
| WBC (10 ⁹ /L) — mean±sd (range) | 6.84±3.07 (3.65-12.74) | 5.19±0.72 (3.96-5.92) |
| Lymphocyte (10 ⁹ /L) — mean±sd (range) | 1.11±0.61 (0.29-2.28) | 1.00±0.49 (0.17-1.85) |
| D-dimer (mg/L) — mean±sd (range) | 2.35±2.91 (0.19-6.84) | 1.54±2.86 (0.17-8.43) |
| Increase in level of D-dimer — no. (%) | 4 (33.3%) | 2 (20.0%) |
| Respiratory pathogens | | |
| The nucleic acid of COVID-19 — no. (%) | 12(100.0%) | 10(100.0%) |
| Unilateral pneumonia — no. (%) | 0 | 0 |
| Bilateral pneumonia — no. (%) | 12(100.0%) | 10(100.0%) |
| Comorbidities | | |
| Diabetes mellitus — no. (%) | 2(16.7%) | 1(10.0%) |
| Cardiovascular disease — no. (%) | 1(8.3%) | 3(50.0%) |
| Cerebrovascular disease — no. (%) | 1(8.3%) | 1(10.0%) |
| Treatment | | |
| Oxygen therapy — no. (%) | 12(100.0%) | 10(100.0%) |
| Mechanical ventilation — no. (%) | 2(16.7%) | 1(10.0%) |
| Antibiotic treatment — no. (%) | 4(33.3%) | 3(30.0%) |
| Antifungal treatment — no. (%) | 0 | 0 |
| Antiviral treatment — no. (%) | 12(100.0%) | 10(100.0%) |
| Glucocorticoids — no. (%) | 12(100.0%) | 10(100.0%) |
| Intravenous Ig therapy — no.(%) | 2(16.7%) | 2(20.0%) |
| Clinical outcome | | |
| Remained in hospital — no. (%) | 4 (33.3%) | 7 (70.0%) |
| Discharged — no. (%) | 7 (58.4%) | 2 (20.0%) |
| Discharged for severe cases— no. (%) | 3 (50.0%) | |
| Discharged for mild cases— no. (%) | 4 (100%) | |
| Died — no. (%) | 1 (8.3%) | 1 (10.0%) |

475

| Table 2. Clinical outcomes of 27 enrolled patients | | | |
|---|--|--|--------------------------------------|
| | Severity of illness — no. (%) | Outcomes (up to 2/26) | Total discharge — no. (%) |
| Dipyridamole group (n=12) | Mild — 4 (33.3%) | 4 discharged (100%) | 7 (58.4%) |
| | Severe — 6 (50.0%) | 3 discharged (50%) 2 in remission (33%) | |
| | Critical ill — 4 (33.3%) | 1 in remission (50%) 1 death (2/09) | |
| Control group (n=10) | Mild — 4 (40.0%) | 3 discharged (75%) | 4 (40.0%) |
| | Severe — 4 (40.0%) | 1 discharged (25%) 1 in remission (25%) | |
| | Critical ill — 2 (20.0%) | 1 death (2/18) | |

476

477

478

479

480

481

482

483

484

485

486

487

488

489

490

Figures and Legends

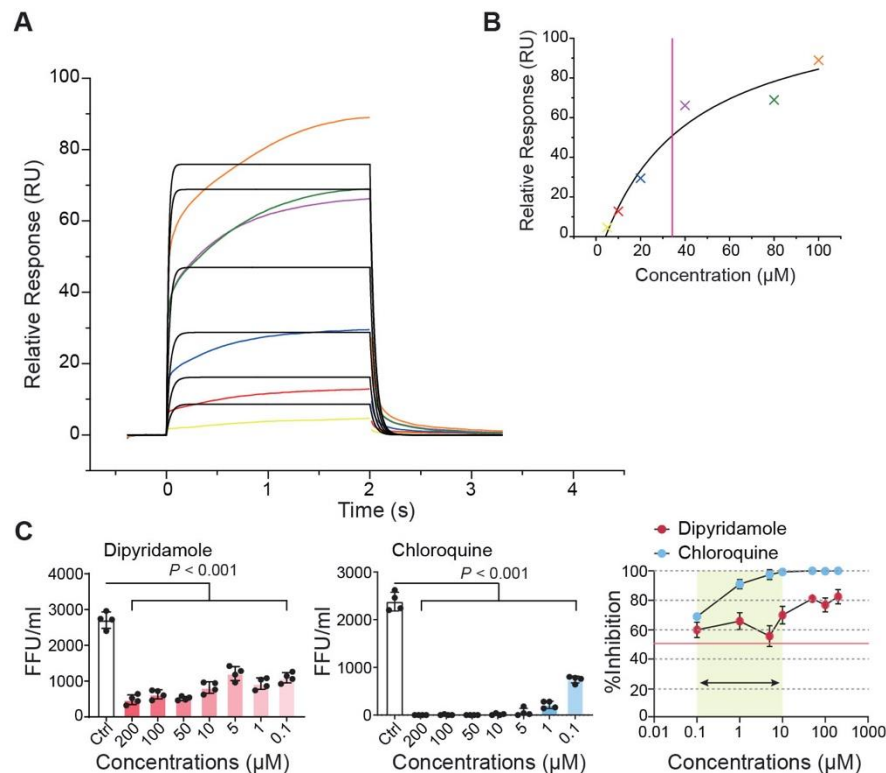


Figure 1. Dipyridamole suppresses Mpro activity by the SPR assay. Experimental SPR sensorgram from Biacore 8K between dipyridamole (DIP) and Mpro, color points overlaid with a 1:1 Langmuir binding model kinetic fit (black). (A) Relative response from injection of DIP at 5, 10, 20, 40, 80, and 100 μM . Global analysis of the shape of the response curves yielded the parameters of on-rate ($K_{on} = 3.20\text{E}+3$), off-rate ($K_{off} = 2.19\text{E}-1$) and the ratio of K_{off} divided by K_{on} ($K_D = 68 \mu\text{M}$). (B) Equilibrium binding responses plotted versus DIP concentration and fitted to a simple binding isotherm to yield an affinity of 34 μM ($K_{D,eq}$). (C) Suppressive effects of DIP and chloroquine on HCoV-19 replication. P values were calculated by Student's t test.

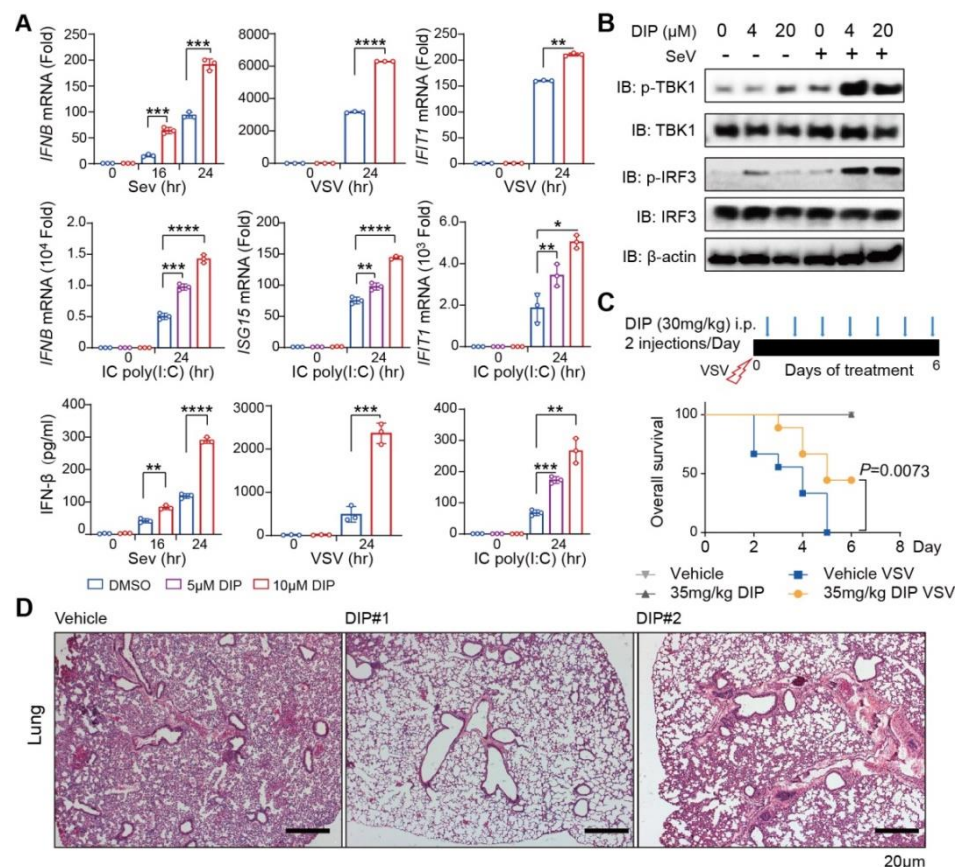


Figure 2. Dipyridamole (DIP) potentiates antiviral immunity to single-stranded RNA viruses. (A) Top, detection of *IFNB* and *IFIT1* mRNA expression in A549 cells treated with or without 5 μM DIP followed by SeV or VSV infection. Middle, real-time PCR detection of *IFNB*, *ISG15* and *IFIT1* mRNA expressions by A549 cells treated with different doses of DIP (0, 5 and 10 μM), followed by intracellular poly (I:C) treatment. Bottom, ELISA detection of IFN-α production by A549 cells. (B) Immunoblot detection of total and phosphorylated (p-) TBK1 and IRF3 in 293T cells with different doses of DIP (0, 4, 20 μM), followed with or without SeV infection. (C) Schematic of the VSV-infection mice model and the survival curve. (D) Histopathology of lungs from mice sacrificed at Day4. Scale bars, 20 μm. Data in A are presented as the means ± SE of at least three biological experiments. P values were calculated by Student's t test, *P < 0.05, ** P < 0.01, *** P < 0.001 and **** P < 0.0001. Data in F are presented with 3 to 9 mice per group, P value was calculated by Log-rank (Mantel-Cox) test (conservative).

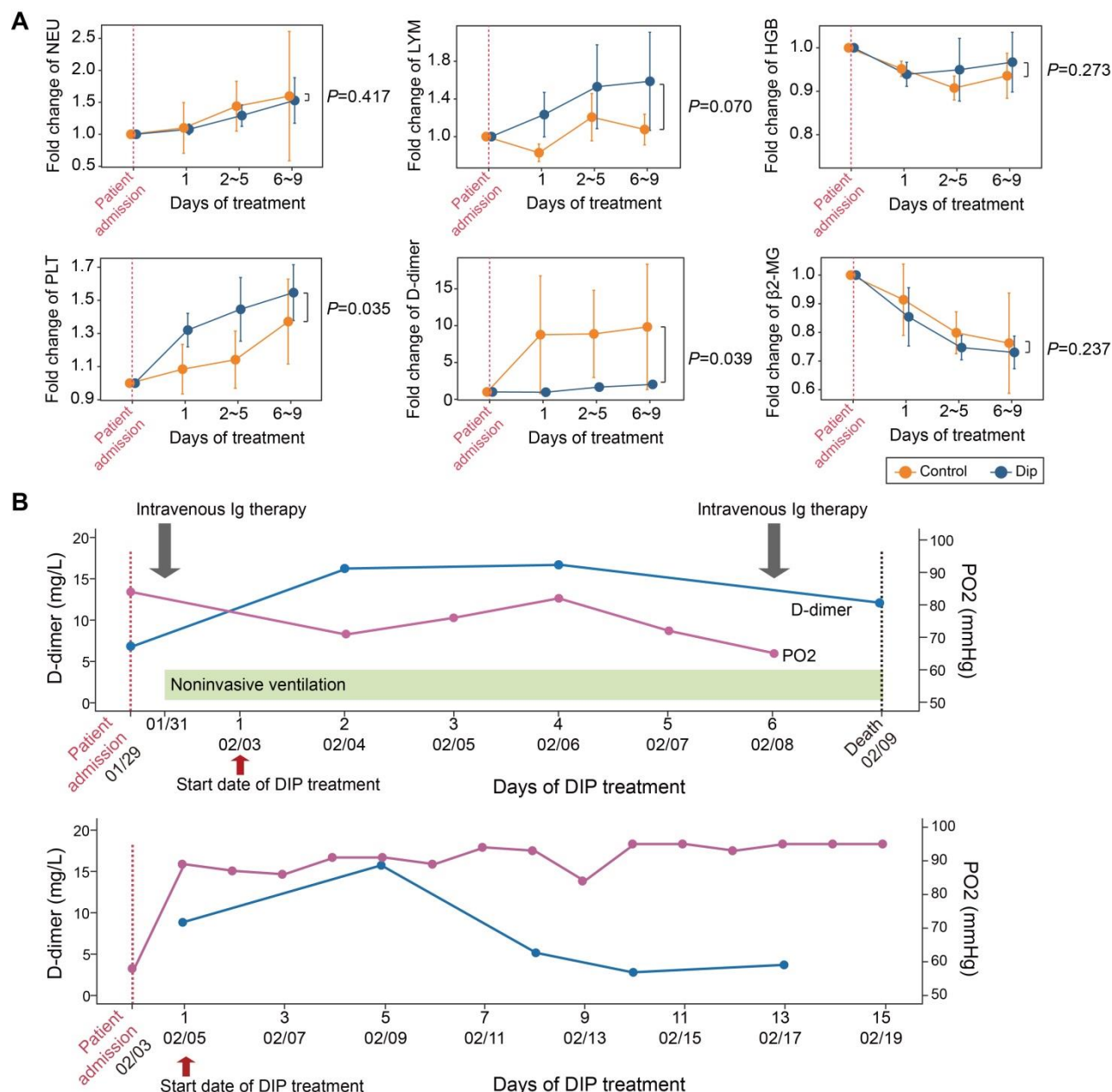


Figure 3. Changes of the study variables during the course of treatment. (A) Dynamic changes in the routine blood indexes (NEU, LYM, HGB, and PLT), coagulation variable (D-dimer), and kidney function indices (β2-MG) in reference to the baseline values. The levels of D-dimer were sustained in DIP treatment group, while those in the control group were significantly increased. Lymphocyte counts were persistently elevated in trend and PLT counts was significantly increased in the DIP group in comparison to the control group. Data are shown as the means ± SE across different

time bins during the treatment course. P values were calculated by Student's t test and indicated beside each panel. (B) Schematics of the treatment overview and clinical parameters of the deceased critically ill patient (top) and the surviving patient (bottom) who received DIP adjunctive therapy.

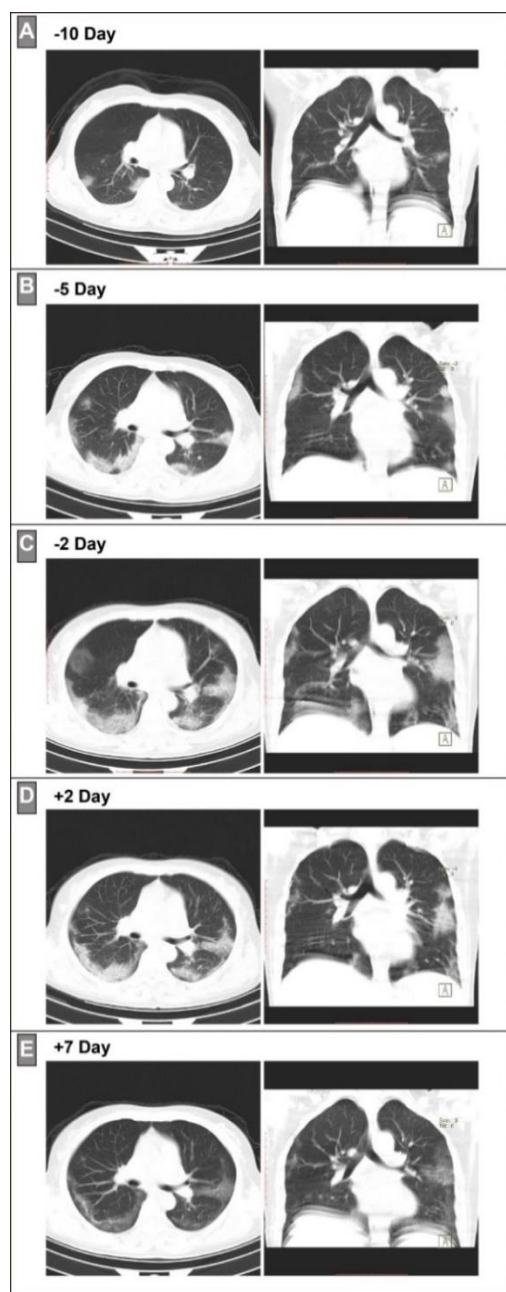


Figure 4. Chest CT images in the axial (left panel) and coronal view (right panel) of represented severe COVID-19 patient before and after receiving DIP adjunctive therapy. (A) Initial chest CT scan 10 days before DIP treatment. (B) Chest CT scan 5 days before DIP treatment. (C) Chest CT scan 2 days before DIP treatment. (D) Chest CT scan 2 days after DIP treatment. (E) Chest CT scan 7 days after DIP treatment.